

Synthesis and Crystal Structure of a First-generation Model for the Trinuclear Copper Site in Ascorbate Oxidase and of a Dinuclear Silver Precursor†

Harry Adams,^a Neil A. Bailey,^a Matthew J. S. Dwyer,^a David E. Fenton,^{*,a}
Paul C. Hellier,^a Paul D. Hempstead^a and Jean Marc Latour^b

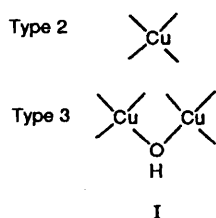
^a Department of Chemistry, The University, Sheffield S3 7HF, UK

^b Laboratoire DRFMC/SESAM/CC, Centre d'Etudes Nucléaires de Grenoble, 85X, 38041 Grenoble Cedex, France

The synthesis and X-ray crystal structure of a disilver complex $[\text{Ag}_2\text{L}^+][\text{BF}_4]_2$ of a bibracchial tetraimine Schiff-base macrocycle derived from the silver-templated cyclocondensation of 2,6-diacetylpyridine and tris(2-aminoethyl)amine are reported. The complex crystallises in the monoclinic space group $P2_1/n$ (a non-standard setting of $P2_1/c$, no. 14) and has unit-cell dimensions $a = 11.660(22)$, $b = 28.14(4)$, $c = 12.158(21)$ Å, $\beta = 107.94(13)^\circ$ with $Z = 4$. Functionalisation of the pendant arms with salicylaldehyde followed by transmetallation with Cu^{II} leads to the formation of a trinuclear copper(II) complex $[\text{Cu}_3\text{L}^{4+}(\text{OH})][\text{ClO}_4]_3 \cdot 2\text{H}_2\text{O}$ in which there is a single Cu^{II} atom 4.9 and 5.9 Å distant from a pair of Cu^{II} atoms which are 3.6 Å apart and hydroxy-bridged. The complex, which crystallises in the monoclinic space group $P2_1$ (no. 4) and has unit cell dimensions $a = 13.997(24)$, $b = 16.043(9)$, $c = 14.353(11)$ Å, $\beta = 118.97(10)^\circ$ with $Z = 2$, may be regarded as a first-generation model for ascorbate oxidase. A study of the magnetic properties shows that the trinuclear copper(II) complex can be regarded as a mononuclear site non-interacting with a moderately coupled copper pair ($2J = -202 \text{ cm}^{-1}$).

Ascorbate oxidase, laccase and ceruloplasmin constitute a group of multi-copper enzymes, known as 'blue' oxidases, which catalyse the one-electron oxidation of the substrate with concomitant four-electron reduction of dioxygen to water.^{1,2} The copper(II) atoms present have been classified according to their spectroscopic properties: Type 1, or blue, has high absorption in the visible region ($\epsilon > 3000 \text{ dm}^3 \text{ mol}^{-1} \text{ cm}^{-1}$ at 600 nm) and an EPR spectrum with $A_{\parallel} < 95 \times 10^{-4} \text{ cm}^{-1}$; Type 2, or normal, has limited absorption and an EPR spectrum typical of small molecule copper(II) complexes ($A_{\parallel} > 140 \times 10^{-4} \text{ cm}^{-1}$); Type 3, which has a strong absorption in the near UV region ($\lambda_{\text{max}} = 330 \text{ nm}$) and no EPR signal is believed to consist of a pair of antiferromagnetically coupled copper(II) ions.^{2,3}

Laccase ($M \approx 65\,000$) is the simplest member of this family and contains four copper(II) atoms (one Type 1, one Type 2 and two Type 3);² dimeric ascorbate oxidase contains eight copper(II) atoms and it was suggested that it was a dimer of two identical laccase-like sub-units.⁴ Cumulative spectroscopic and azide bonding studies on *Rhus vernicifera* laccase led to the proposal that the Type 2 and Type 3 centres defined a trinuclear copper cluster site (I).⁵



The long absence of crystallographic information concerning this type of site was redressed with the publication of an X-ray

diffraction study of oxidised ascorbate oxidase from zucchini.^{6a} Two crystal forms were analysed, one a dimer ($M \approx 140\,000$) and one a tetramer ($M \approx 280\,000$). Each sub-unit has four copper atoms present bound as mononuclear and trinuclear species. The mononuclear copper, bound to two histidines, one cysteine and one methionine ligand, is of Type 1 resembling plastocyanin; this site is isolated from the trinuclear site by ca. 15 Å. The Type 2 copper which is 3.9 Å from one Type 3 copper and 4.0 Å from the second is co-ordinated to two histidine ligands together with a water molecule, or hydroxide anion. The trinuclear site may be subdivided into a Type 2 copper and a pair of Type 3 copper atoms held in an approximately isosceles triangular array. The Type 3 coppers are each co-ordinated by three histidine ligands and form a trigonal prism with an intermetallic separation of 3.4 Å. The X-ray data indicate the existence of an oxo or hydroxo bridging ligand. The identification of the trinuclear site thus provides confirmation of the earlier proposals from solution studies.

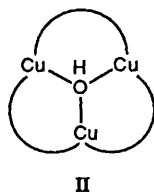
The structure has recently been further refined at 1.9 Å resolution leading to intermetallic separations of 3.66 and 3.78 Å (Type 2–Type 3) and 3.68 Å (Type 3–Type 3) in subunit A and 3.69 and 3.90 Å (Type 2–Type 3) and 3.73 Å (Type 3–Type 3) in subunit B.^{6b} The existence of a central oxygen ligand would give rise to five-co-ordination of both of the Type 3 copper atoms and square planar geometry for the Type 2 copper atom,⁵ and EPR studies on Type 2-depleted and reconstructed laccase have suggested that there is a central water molecule that could point towards the Type 3 pair and bridge with the Type 2 atom.⁷ However if there is such an oxygen atom it is not seen in the X-ray structure and the Fourier difference map does not show any significant density that could correspond with such a molecule. Although this structural revision has occurred comparison with the original report is adhered to as this was the basis for the generation of our model.

Modelling studies based on the spatial structure of ascorbate oxidase have allowed an assignment of the amino acid sequences of laccase and ceruloplasmin to be made.⁸ From this

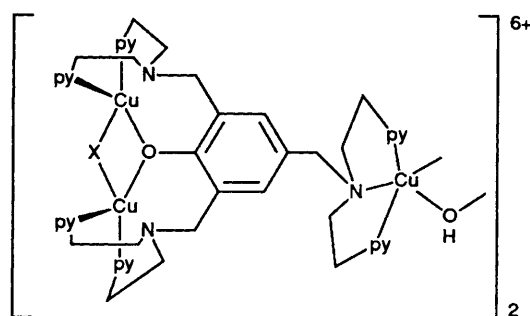
† Supplementary data available: see Instructions for Authors, *J. Chem. Soc., Dalton Trans.*, 1993, Issue 1, pp. xxiii–xxviii.

the proposal has been made that laccase has one mononuclear copper atom and a trinuclear centre located similarly to that in ascorbate oxidase; ceruloplasmin has three mononuclear copper atoms and one trinuclear centre.

Synthetic analogues for the trinuclear site in ascorbate oxidase and the related 'blue' oxidases are not very evident. There are numerous examples in the literature⁹ of hydroxo-bridged trinuclear copper(II) complexes, depicted schematically below (II). They are mostly based on equilateral triangles of



copper atoms with intermetallic distances close to 3.0 Å and supported by at least one μ_3 -hydroxo bridge; there is a single complex derived from a polytopic macrocyclic ligand which has a double μ_3 -hydroxo bridge.¹⁰ One hexanuclear copper(II) complex, derived from a poly podal ligand (III, X = N₃), has



X = OH or N₃, py = 2-pyridyl

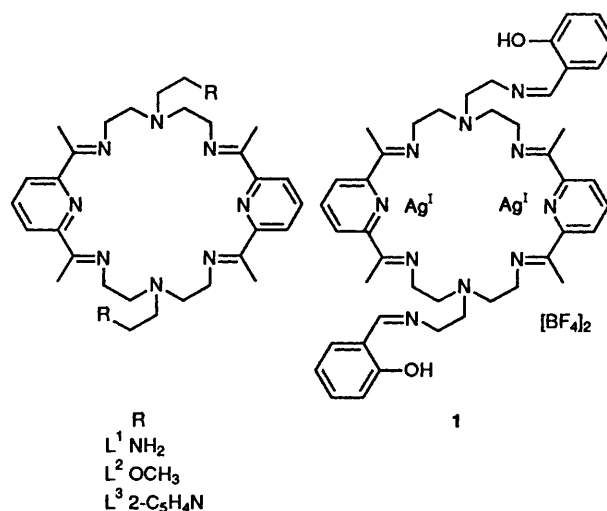
been reported.¹¹ There are two approximately isosceles triangular arrays of copper(II) atoms present and each has a Type 3-like pair of copper atoms having a 3.11 Å separation supported by an endogenous phenoxo-bridge derived from the ligand; the third copper is distant from the pair by 7.78 and 7.46 Å respectively.

We have earlier reported structural studies on mononuclear barium and dinuclear silver(I) complexes of a series of bi-bracchial tetraimine Schiff-base macrocycles, L¹-L³, which have shown that the macrocycles fold to present molecular clefts into which the metal ions co-ordinate.¹² This mode of metal incorporation is not dissimilar to that of the metalloproteins in which the requisite metal is bound in a pocket or cleft produced by the conformational arrangement of the protein. Investigation of the structures suggested that suitable modification of the pendant arms would lead to the opportunity to synthesise trinuclear metal complexes and we here report the intentional synthesis and the crystal structure of a trinuclear copper(II) complex, derived from the disilver(I) complex [Ag₂(H₂L⁴)]-[BF₄]₂ **1** via transmetallation, which serves as a first-generation model for the trinuclear site in ascorbate oxidase and related 'blue' copper oxidases. A preliminary account of the X-ray crystal structure of the trinuclear copper(II) complex [Cu₃L⁴-(OH)]-[ClO₄]₃·2H₂O has been presented.¹³

Experimental

The microanalytical, magnetic and spectroscopic data were recorded as previously reported.^{12,14}

Reaction of Tris(2-aminoethyl)amine with 2,6-Diacetylpyridine in the Presence of Silver(I) Ions.—The experimental



procedure for the metal-templated cyclocondensation reactions was previously described in ref. 12.

[Ag₂L¹][BF₄]₂ **2**. Yield 44%, m.p. 196 °C (decomp.). IR (KBr disc): ν_{NH_2} 3371, 3315, $\nu_{\text{C=N}}$ 1641 cm⁻¹. Mass spectrum [positive ion (+ve) fast-atom bombardment (FAB)]: *m/z* 849 [Ag₂L¹(BF₄)₂]⁺ [Found (required for C₃₀H₄₆Ag₂B₂F₈N₁₀): C, 38.45 (38.45); H, 5.00 (4.95); N, 14.85 (15.10%)]. ¹³C NMR (CD₃CN): δ 170.7, 164.2, 154.7, 150.9, 140.3, 125.4, 124.7, 57.6, 55.1, 53.4, 53.1, 48.0, 40.2, 18.4, 16.3.

[Ag₂L¹][ClO₄]₂ **3**. Yield 72%. IR (KBr disc): ν_{NH_2} 3380, 3323, $\nu_{\text{C=N}}$ 1641 cm⁻¹. Mass spectrum (+ve FAB): *m/z* 862 [Ag₂L¹(ClO₄)₂]⁺ [Found (required for C₃₀H₄₆Ag₂Cl₂N₁₀O₈): C, 37.20 (37.50); H, 4.80 (4.80); Cl, 7.55 (7.35); N, 14.50 (14.55%)]. ¹³C NMR (CD₃CN): δ 170.6, 164.1, 154.5, 150.8, 140.3, 125.4, 124.6, 57.5, 54.9, 53.3, 53.0, 47.9, 40.1, 18.3, 16.2.

Transmetallation Reactions of the Disilver(I) Complexes 2 and 3 with Copper(II) Salts.—The experimental procedure followed was the same as that described previously for the transmetalation reactions in ref. 15.

[Cu₂L¹][BF₄]₄·3H₂O **4**. Yield 88%, m.p. 243 °C (decomp.). IR (KBr disc): $\nu_{\text{C=N}}$ 1667 cm⁻¹. Mass spectrum (+ve FAB): *m/z* 934 [Cu₂L¹(BF₄)₃]⁺ [Found (required for C₃₀H₅₂B₄Cu₂F₁₆N₁₀O₃): C, 33.65 (33.50); H, 4.65 (4.85); N, 13.05 (13.05%)].

[Cu₂L¹][ClO₄]₄·2H₂O **5**. Yield 90%. IR (KBr disc): $\nu_{\text{C=N}}$ 1666 cm⁻¹. Mass spectrum (+ve FAB): *m/z* 971 [Cu₂L¹(ClO₄)₃]⁺ [Found (required for C₃₀H₅₀Cl₄Cu₂N₁₀O₁₈): C, 32.30 (32.55); H, 4.00 (4.55); Cl, 12.75 (12.80); N, 12.40 (12.65%)].

Functionalisation of the Disilver(I) Complex 2 with Salicylaldehyde.—A solution of salicylaldehyde (4 mmol) in methanol (100 cm³) was added dropwise to a refluxing methanolic solution (200 cm³) of [Ag₂L¹][BF₄]₂ **2**. The reaction mixture was heated at reflux temperature for 18 h and filtered hot to remove the product [Ag₂(H₂L⁴)]-[BF₄]₂ **1** as a pale yellow powder which was recrystallised from acetonitrile. Yield 26%, m.p. 200 °C (decomp.). IR (KBr disc): $\nu_{\text{C=N}}$ 1627 cm⁻¹. Mass spectrum (+ve FAB): *m/z* 1057 [Ag₂(H₂L⁴)(BF₄)₂]⁺ [Found (required for C₄₄H₅₄Ag₂B₂F₄N₁₀O₂): C, 46.30 (46.20); H, 4.65 (4.75); N, 12.45 (12.25%)]. ¹³C NMR [(CD₃)₂SO]: δ 165.3, 163.3, 158.0, 149.5, 140.2, 132.8, 126.6, 124.0, 120.5, 115.9, 58.0, 56.7, 54.9, 47.7, 15.9.

Transmetalation of the Functionalised Pendant-armed Complex 1 with Copper(II).—A suspension of the disilver macrocyclic complex **1** (0.35 mmol) in methanol (100 cm³) was heated until reflux temperature was attained. Acetonitrile (ca. 15 cm³) was then added until all the complex had dissolved. A solution of copper(II) acetate monohydrate (0.35 mmol) in methanol (40

Table 1 Crystal structure data

Compound	2	6
Formula	C ₃₀ H ₄₆ Ag ₂ B ₂ F ₈ N ₁₀	C ₄₄ H ₅₇ Cl ₃ Cu ₃ N ₁₀ O ₁₇
M _r	936.11	1294.96
Crystal dimensions/mm	0.475 × 0.25 × 0.20	0.4 × 0.3 × 0.1
Crystal appearance	Yellow blocks	Dark green rectangular prism
Space group	P2 ₁ /n [a non-standard setting of P2 ₁ /c (no. 14)]	P2 ₁ (no. 4)
a/Å	11.660(22)	13.997(24)
b/Å	28.14(4)	16.043(9)
c/Å	12.158(21)	14.353(11)
β/°	107.94(13)	118.97(10)
U/Å ³	3795(10)	2820(6)
Z	4	2
D _c (D _m)/g cm ⁻³	1.638	1.525 (1.56)
μ/cm ⁻¹	10.96	13.39
F(000)	1887.64	1329.72
h,k,l ranges	0–14, 0–35, –15 to 15	0–17, 0–20, –18 to 18
No. unique reflections observed (measured)	3252 (7228)	1744 (5167)
Criterion	F _o /σ(F _o) > 3.0	F _o /σ(F _o) > 4.0
R _σ	0.0836	0.0842
Min., max. transmission coefficients	0.353, 0.397	0.639, 0.803
No. of parameters	493	257
R ^a	0.0974	0.1044
R' (g) ^b	0.0677 (0.000 25)	0.0914 (0.0015)
Max., min. residual peaks in final Fourier difference map/e Å ⁻³	+1.11, –0.90	0.78, –0.75

Details in common: crystal system, monoclinic; absorption correction, 8 ψ scans. ^a R = Σ|Δ|/ΣF_o. ^b R' = Σw³|Δ|/Σw³F_o where |Δ| = |F_o – F_c|; weighting scheme, w⁻¹ = σ²(F) + gF².

cm³) was added dropwise followed by a methanolic solution (25 cm³) of copper(II) tetrafluoroborate hexahydrate (0.70 mmol). After heating at reflux temperature for 2 h the reaction mixture was filtered hot into a solution of sodium perchlorate (3.5 mmol) in methanol (20 cm³). The product, [Cu₃L⁴(OH)]-[ClO₄]₃·2H₂O **6**, precipitated as dark green crystals on cooling. Yield 71%. IR (KBr disc): ν_{C=N} 1631 cm⁻¹. Mass spectrum (+ve FAB): m/z 1159 [Cu₃L⁴(OH)(ClO₄)₂]⁺ [Found (required for C₄₄H₅₇Cl₃Cu₃N₁₀O₁₇): C, 40.25 (40.80); H, 4.55 (4.45); Cl, 8.35 (8.20); N, 10.65 (10.80%)].

X-Ray Data Collection, Solution and Refinement for Complexes 2 and 6.—Three-dimensional, room-temperature X-ray data were collected in the range 3.5 < 2θ < 50° on a Nicolet R3 4-circle diffractometer by the omega scan method using graphite-monochromated Mo-Kα radiation (λ = 0.710 69 Å). The structures were solved by Patterson and Fourier techniques and refined by blocked cascade least-squares methods. Complex scattering factors were taken from ref. 16 and from the program package SHELXTL¹⁷ as implemented on the Data General Nova 3 computer, which was used for structure solution and refinement. The crystal structure data are listed in Table 1.

For the disilver complex **2** both tetrafluoroborate anions were found to be disordered, and a model with two interpenetrating disorder components for each anion was refined with constrained T_d symmetry for each component: occupancy parameters refined to 0.67/0.33 and 0.81/0.19. Hydrogen atoms were included in calculated positions, with isotropic thermal parameters related to those of the supporting atom, and refined in riding mode. Refinement converged at a final R 0.0974 [493 parameters, maximum shift/estimated standard deviation (e.s.d.) 0.386], with allowance for the thermal anisotropy of all non-hydrogen atoms, with the exception of the eight fluorine atoms of lower occupancy, and of the boron atoms.

For the trinuclear complex **6** the unco-ordinated water molecule was equally disordered between two mutually incompatible sites. The perchlorate anions were modelled with Cl–O taken as approximately 1.4 Å; the anions were finally refined as rigid groups. The chlorine atoms of the second perchlorate were constrained to be coincident; for the perchlorates based on Cl(1a), Cl(1b) and Cl(2) the site occupancies of the fragments

did not differ significantly from 0.5 and hence were fixed at this value. Perchlorates based on Cl(3a) and Cl(3b) refined to occupancies of 0.75 and 0.25 respectively. Anisotropic thermal parameters were applied only to the three copper atoms and the full-occupancy chlorine atom, Cl(2).

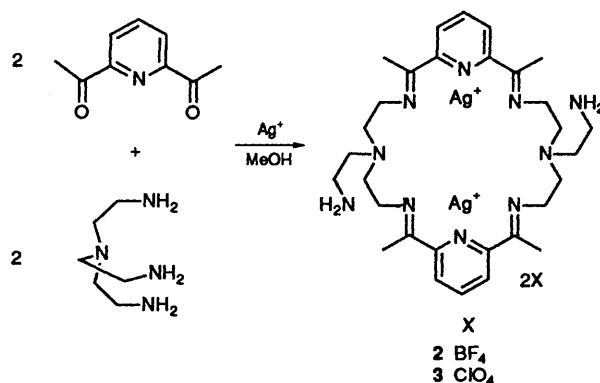
Atomic positional parameters with estimated standard deviations are listed in Tables 2 and 3.

Additional material available from the Cambridge Crystallographic Data Centre comprises H-atom coordinates, thermal parameters and remaining bond lengths and angles.

Results and Discussion

The diprimary amine pendant-armed macrocycle L¹ was first prepared *via* the barium(II)-templated [2 + 2] cyclocondensation of tris(2-aminoethyl)amine (tren) and 2,6-diacetylpyridine.¹⁸ It has been shown that, as a result of their large ionic radius (1.26 Å) and stereochemical flexibility, silver(I) ions are effective in promoting the formation of similar Schiff-base macrocycles.¹⁹ Thus the potential of silver(I) to act as an alternative template in the synthesis of L¹ was investigated and found to result in the formation of the dinuclear complexes **2** and **3** (Scheme 1).

It has been noted previously that reaction of tren with

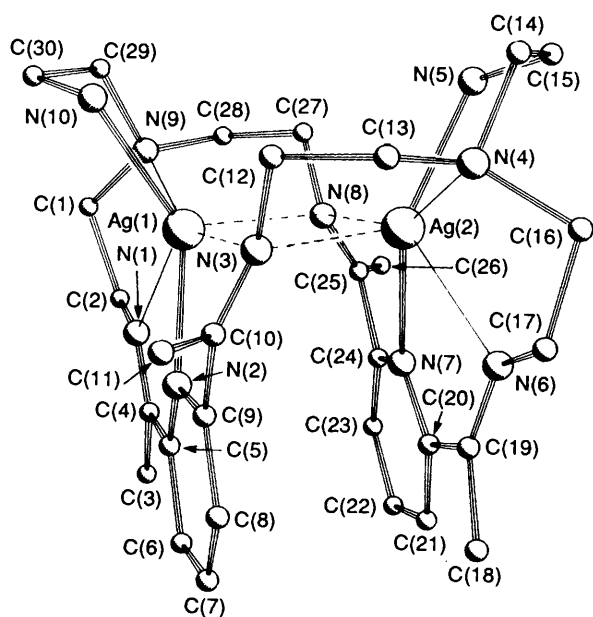


Scheme 1 Metal-ion templated synthesis of the diprimary amine pendant-armed macrocycle L¹

Table 2 Atomic coordinates ($\times 10^4$) for $[\text{Ag}_2\text{L}^1][\text{BF}_4]_2$ **2** with estimated standard deviations (e.s.d.s) in parentheses*

Atom	x	y	z	Atom	x	y	z
Ag(1)	1365(1)	1064(1)	-844(1)	C(20)	2165(11)	1457(5)	3063(11)
Ag(2)	1971(1)	1999(1)	675(1)	C(21)	2563(14)	1120(6)	3981(11)
N(1)	2142(9)	290(4)	5(9)	C(22)	3504(15)	810(6)	4024(15)
N(2)	399(9)	792(4)	469(9)	C(23)	4080(12)	847(5)	3195(11)
N(3)	-258(10)	1694(4)	-465(9)	C(24)	3638(12)	1179(5)	2299(12)
N(4)	470(10)	2707(4)	171(10)	C(25)	4254(12)	1242(4)	1365(12)
N(5)	2896(10)	2572(4)	-100(10)	C(26)	5612(11)	1149(5)	1773(12)
N(6)	1169(9)	2170(4)	2309(10)	C(27)	4141(11)	1420(5)	-575(12)
N(7)	2708(9)	1468(4)	2234(8)	C(28)	4263(11)	963(5)	-1162(11)
N(8)	3585(9)	1363(4)	350(9)	C(29)	2563(12)	873(5)	-2949(11)
N(9)	3067(10)	731(4)	-1703(9)	C(30)	1170(12)	843(5)	-3420(12)
N(10)	608(10)	1174(4)	-2825(9)	B(1)	6630(2)	2528(1)	1436(4)
C(1)	3088(13)	222(5)	-1550(12)	F(1)	7280(4)	2203(2)	2208(9)
C(2)	3159(12)	76(5)	-299(12)	F(2)	5641(2)	2658(1)	1736(2)
C(3)	2546(15)	-226(5)	1761(13)	F(3)	6273(6)	2334(3)	357(7)
C(4)	1903(13)	167(5)	917(11)	F(4)	7325(3)	2918(1)	1444(3)
C(5)	872(12)	435(5)	1162(12)	B(1a)	6742(1)	2474(1)	1584(1)
C(6)	486(15)	300(6)	2102(13)	F(1a)	7419(2)	2089(1)	2072(2)
C(7)	-433(16)	559(7)	2311(15)	F(2a)	6990(13)	2596(4)	597(9)
C(8)	-930(13)	926(5)	1578(14)	F(3a)	7010(13)	2845(2)	2340(7)
C(9)	482(12)	1051(6)	674(13)	F(4a)	5550(1)	2364(3)	1327(15)
C(10)	-1008(12)	1441(5)	-132(12)	B(2)	7745(1)	468(1)	4925(1)
C(11)	-2367(12)	1516(6)	-498(15)	F(5)	8056(6)	731(2)	5914(3)
C(12)	-685(13)	2103(6)	-1228(13)	F(6)	8482(2)	82(1)	5069(2)
C(13)	-760(13)	2564(6)	-584(14)	F(7)	7863(7)	738(2)	4035(5)
C(14)	1033(15)	3038(6)	-434(14)	F(8)	6580(1)	321(1)	4681(8)
C(15)	2416(15)	3038(5)	18(13)	B(2a)	7556(18)	486(10)	4843(14)
C(16)	414(14)	2912(5)	1274(13)	F(5a)	6702(2)	321(1)	3882(2)
C(17)	256(13)	2541(5)	2114(13)	F(6a)	7026(40)	770(16)	5455(28)
C(18)	335(13)	743(5)	3686(12)	F(7a)	8393(28)	742(18)	4521(37)
C(19)	1190(12)	1812(5)	2991(11)	F(8a)	8105(39)	113(17)	5513(28)

* Atoms [B(1), F(1)–F(4)], [B(1a), F(1a)–F(4a)], [B(2), F(5)–F(8)], [B(2a), F(5a)–F(8a)] comprise components of the disordered tetrafluoroborate groups with occupancies 0.67, 0.33, 0.81 and 0.19 respectively.

**Fig. 1** Molecular structure of the $[\text{Ag}_2\text{L}^1]^{2+}$ dication in complex **2**

aromatic and heterocyclic dicarbonyls leads to the facile generation of Schiff-base macrobicycles both *via* metal-templated and *via* non-template procedures.²⁰ The non-macrobicyclic nature of **2** and **3** is evidenced from their IR spectra in which the presence of unreacted primary amine groups is indicated by the appearance of two strong peaks between 3280 and 3380 cm^{-1} , assigned to the symmetric and asymmetric NH_2 stretching modes. An intense absorption around 1640 cm^{-1} arises from

the stretching vibration of the imino $\text{C}=\text{N}$ bonds. The products were further characterised by positive ion FAB mass spectrometry (major peaks at m/z 849 and 862 corresponding to cations generated *via* the loss of a single counter ion from **2** and **3** respectively).

Recrystallisation of **2** from methanol yielded yellow blocks suitable for X-ray crystallography. The structure of the dication (Fig. 1) shows approximate, but not imposed, C_2 symmetry with the two six-co-ordinate silver ions bound in the pyridine diimine head units of the macrocycle separated by 3.167 Å. The two imino nitrogen atoms within each pyridine diimine fragment show different co-ordination modes. One of the nitrogens acts as a bridge between the two silver ions whilst the other is bound only to a single ion. The shortest interactions shown by each silver ion are to the pyridyl nitrogen and to the primary amine on the pendant arm (2.30–2.36 Å). There are intermediate interactions to a non-bridging imino nitrogen donor (2.46 and 2.49 Å) and to the tertiary amines (2.68 and 2.60 Å), whilst the longest bonds are to the bridging imino nitrogens (2.68–2.73 Å). The most obvious deviation from C_2 symmetry occurs in the two silver–tertiary nitrogen bond lengths. The bond lengths and angles defining the co-ordination geometry around each silver ion are presented in Table 4.

The overall conformation of the macrocyclic dication is folded so as to form a cleft with the metal atoms well hidden at one end. The angle between the mean planes through the pyridyl fragments [root mean square (r.m.s.) deviations 0.011 and 0.015 Å] is only 5°, and their planes lie 3.48 Å apart, although the aromatic fragments do not lie face-to-face, but are laterally displaced. The silver atoms lie 0.387 and 0.117 Å from the pyridyl planes. In order that two imino nitrogen atoms may achieve bridging positions, they are twisted out of the pyridyl planes to greater extents [torsion angles $\text{N}(2)\text{--C}(9)\text{--C}(10)\text{--N}(3)$ –42°, $\text{N}(7)\text{--C}(24)\text{--C}(25)\text{--N}(8)$ –34°] than are the non-

Table 3 Atomic coordinates ($\times 10^4$) for $[\text{Cu}_3\text{L}^4(\text{OH})][\text{ClO}_4]_3 \cdot 2\text{H}_2\text{O} \cdot 6$ with e.s.d.s in parentheses*

Atom	x	y	z	Atom	x	y	z
Cl(1a)	5349(16)	728(14)	452(15)	C(9)	1642(28)	1983(19)	-739(24)
O(11a)	5092	-116	429	N(3)	1558(18)	2909(15)	-881(17)
O(12a)	5961	991	1508	C(10)	515(23)	3196(21)	-1773(22)
O(13a)	5957	845	-76	C(11)	-399(27)	3002(24)	-1554(24)
O(14a)	4386	1194	-55	N(4)	32(19)	3072(15)	-456(18)
Cl(1b)	5056(17)	649(13)	-111(17)	C(12)	-472(26)	2749(21)	18(24)
O(11b)	5904	1103	-120	C(13)	-1589(27)	2372(24)	-536(26)
O(12b)	4310	410	-1150	N(5)	1248(17)	2763(13)	1594(15)
O(13b)	5483	-60	523	C(14)	144	2747	1278
O(14b)	4529	1144	303	C(15)	-309	2726	1910
Cl(2)	2683(8)	-1688(7)	4724(8)	C(16)	394	2733	3014
O(21a)	2978	-2466	5224	C(17)	1573	2875	3401
O(22a)	3260	-1063	5462	C(18)	1958	2789	2683
O(23a)	2933	-1660	3892	C(19)	3087(27)	2710(22)	3074(25)
O(24a)	1563	-1565	4318	C(20)	3777(28)	3388(25)	3821(26)
O(21b)	3254	-1834	4166	N(6)	3429(22)	2166(19)	2729(22)
O(22b)	2396	-2450	4994	C(21)	4554(33)	2005(29)	2908(34)
O(23b)	3345	-1239	5651	C(22)	5005(34)	1342(26)	3512(32)
O(24b)	1739	-1230	4085	N(7)	4452(22)	554(18)	3272(21)
Cl(3a)	-2826(14)	-2702(12)	3674(13)	C(23)	4792(26)	-5(24)	2734(25)
O(31a)	-3228	-3259	2819	C(24)	3974(28)	-779(22)	2225(24)
O(32a)	-2698	-1916	3331	N(8)	3546(21)	-855(17)	1105(19)
O(33a)	-1818	-2985	4479	C(25)	3876(26)	-1460(24)	735(23)
O(34a)	-3563	-2649	4068	C(26)	4561(29)	-2198(24)	1346(27)
Cl(3b)	-2368(44)	-1461(39)	3888(39)	C(27)	2570(26)	3252(22)	-852(24)
O(31b)	-3253	-1756	3989	C(28)	3507(24)	3486(23)	260(21)
O(32b)	-2752	-980	2963	N(9)	2998(19)	3903(15)	848(18)
O(33b)	-1769	-2135	3825	C(29)	3471(25)	4526(19)	1360(22)
O(34b)	-1698	-972	4773	C(30)	3038(17)	5030(12)	1864(15)
Cu(1)	2606(3)	0	-22(3)	C(31)	3750	5737	2495
Cu(2)	2736(3)	838(3)	2379(3)	C(32)	3388	6265	3031
Cu(3)	1526(3)	3487(3)	377(3)	C(33)	2413	6103	3049
O(H1)	2819(13)	788(12)	1031(12)	C(34)	1651	5436	2331
O(S1)	978(18)	-247(14)	-132(16)	C(35)	2011	4945	1751
O(S2a)	210(82)	3785(67)	5131(77)	O(1)	1267(16)	4441(13)	1128(15)
O(S2b)	-384(77)	2170(66)	5296(72)	C(36)	4559(31)	177(27)	4286(27)
N(1)	2735(16)	-863(12)	-963(15)	C(37)	3868(30)	627(29)	4655(29)
C(1)	3358	-1506	-401	N(10)	2749(22)	678(19)	3742(20)
C(2)	3442	-2076	-1096	C(38)	1909(24)	600(20)	3880(24)
C(3)	2993	-1988	-2205	C(39)	793(13)	630(14)	3021(13)
C(4)	2352	-1187	-2720	C(40)	-100	490	3284
C(5)	2217	-612	-1917	C(41)	-1189	483	2523
C(6)	1737(27)	210(23)	-2336(27)	C(42)	-1468	578	1337
C(7)	1094(30)	421(25)	-3458(26)	C(43)	-648	546	1172
N(2)	1827(20)	655(18)	-1529(19)	C(44)	485	638	1902
C(8)	1380(27)	1511(21)	-1771(23)	O(2)	1196(16)	700(14)	1543(15)

* Estimated standard deviations not quoted for non-pivotal atoms of constrained groups.

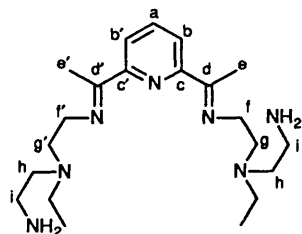
Table 4 Co-ordination geometry about atoms Ag(1) and Ag(2) in complex **2**; bond lengths in Å, other entries are the angles ($^\circ$) subtended at silver by the nitrogen atoms in the first column and the bottom row

Ag(1)-N(1)	2.462(11)						
Ag(1)-N(2)	2.347(13)	67.5(4)					
Ag(1)-N(3)	2.733(13)	133.5(4)	66.1(4)				
Ag(1)-N(8)	2.684(10)	83.2(3)	108.6(3)	107.9(3)			
Ag(1)-N(9)	2.680(13)	68.4(4)	136.0(4)	157.9(4)	67.3(3)		
Ag(1)-N(10)	2.316(11)	121.8(4)	129.9(4)	91.5(4)	121.0(4)	74.5(4)	
		N(1)	N(2)	N(3)	N(8)	N(9)	
Ag(2)-N(3)	2.682(11)						
Ag(2)-N(4)	2.596(12)	69.4(4)					
Ag(2)-N(5)	2.297(13)	121.0(4)	74.5(4)				
Ag(2)-N(6)	2.489(14)	86.1(4)	69.4(4)	122.1(4)			
Ag(2)-N(7)	2.359(10)	105.5(4)	136.7(4)	132.4(4)	67.3(4)		
Ag(2)-N(8)	2.713(12)	108.6(3)	156.7(4)	88.2(4)	133.8(4)	66.5(4)	
		N(3)	N(4)	N(5)	N(6)	N(7)	

bridging imines [torsion angles $\text{N}(1)-\text{C}(4)-\text{C}(5)-\text{N}(2) -6^\circ$, $\text{N}(6)-\text{C}(19)-\text{C}(20)-\text{N}(7) -17^\circ$]. Bond lengths in the macrocycle are all unexceptional and there are no noteworthy intermolecular contacts.

The NMR spectral data for **2** are consistent with the macrocycle adopting a solution conformation similar to that determined in the solid state wherein the C_2 symmetry reflects the different co-ordination modes of the two imino nitrogen donors

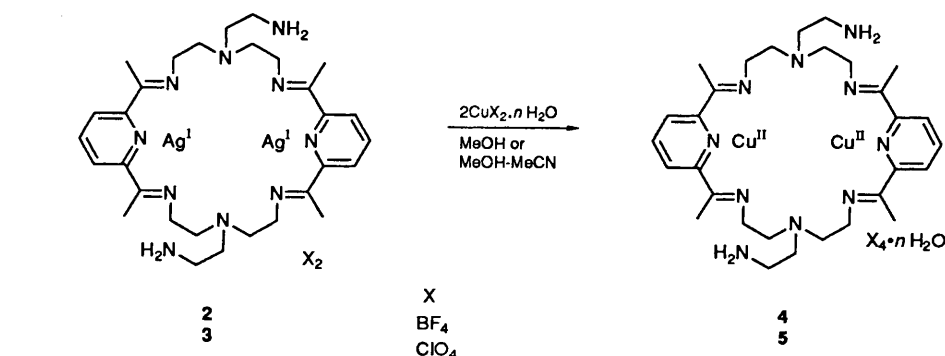
on each pyridine diimine fragment. In the crystal structure one nitrogen is bound to a single silver ion whilst the other acts as a bridge between both the silvers (Fig. 1). The ^{13}C NMR spectrum of **2** shows two separate signals for each carbon atom, except for those arising from the *para*-pyridine [$\delta_{\text{C}}(\text{C}_a)$ 140.3] and pendant arm [e.g. $\delta_{\text{C}}(\text{C}_i)$ 40.2] carbon atoms. This is shown clearly by the *meta*-pyridine [$\delta_{\text{C}}(\text{C}_b, \text{C}_b')$ 125.4, 124.7], *ortho*-pyridine [$\delta_{\text{C}}(\text{C}_c, \text{C}_c')$ 154.7, 150.9], imino [$\delta_{\text{C}}(\text{C}_d, \text{C}_d')$ 170.7, 164.2] and methyl [$\delta_{\text{C}}(\text{C}_e, \text{C}_e')$ 18.4, 16.3] carbon resonances. These signals may be attributed to the molecule retaining C_2 symmetry in solution.



The ^1H NMR spectrum may be similarly interpreted; two doublets [$\delta_{\text{H}}(\text{H}_b, \text{H}_b')$ 7.90, 7.84, $^3J(\text{H}_a-\text{H}_b, \text{H}_b')$ 8 Hz] are detected reflecting the inequivalence of the *meta*-pyridine positions on each ring together with two methyl signals [$\delta_{\text{H}}(\text{H}_e, \text{H}_e')$ 2.31, 2.02] which demonstrate the inequivalence of the two methyl environments. This is further illustrated by their different multiplicities; whereas the former is a singlet, the latter

Table 5 Proton NMR spectral assignments for $[\text{Ag}_2\text{L}^1][\text{BF}_4]_2$ **2** in CD_3CN

Atom	δ_{H} (multiplicity)	Coupling constants/Hz
H_a	7.92 (t)	$^3J(\text{H}_a-\text{H}_b, \text{H}_b') = 8$
H_b and H_b'	7.90 (dd), 7.84 (dd)	$^4J(\text{H}_b-\text{H}_b') = 1$
H_c	2.31 (s)	$^2J(\text{H}_{\text{r}\alpha}-\text{H}_{\text{r}\beta}) = 11.5$
$\text{H}_{\text{r}\alpha}$	3.92 (td)	$^3J(\text{H}_{\text{r}\alpha}-\text{H}_{\text{g}\alpha}) = 2.5$
$\text{H}_{\text{r}\beta}$	3.52 (dt)	$^3J(\text{H}_{\text{r}\alpha}-\text{H}_{\text{g}\beta}) = ca. 12$
$\text{H}_{\text{g}\alpha}$	ca. 2.72 (dm)	$^3J(\text{H}_{\text{r}\alpha}-\text{H}_{\text{g}\alpha}) = 2.5$
$\text{H}_{\text{g}\beta}$	ca. 2.91 (tm)	$^3J(\text{H}_{\text{r}\beta}-\text{H}_{\text{g}\beta}) = 2.5$
H_c'	2.02 (t)	$^5J(\text{H}_c-\text{H}_{\text{r}\alpha}, \text{H}_{\text{r}\beta}) = 1.25$
$\text{H}_{\text{r}\alpha}'$ and $\text{H}_{\text{r}\beta}'$	3.32 (m)	
$\text{H}_{\text{g}\alpha}'$ and $\text{H}_{\text{g}\beta}'$	ca. 2.44 (m), 2.85 (m)	
H_h and H_i	3.0–2.6	



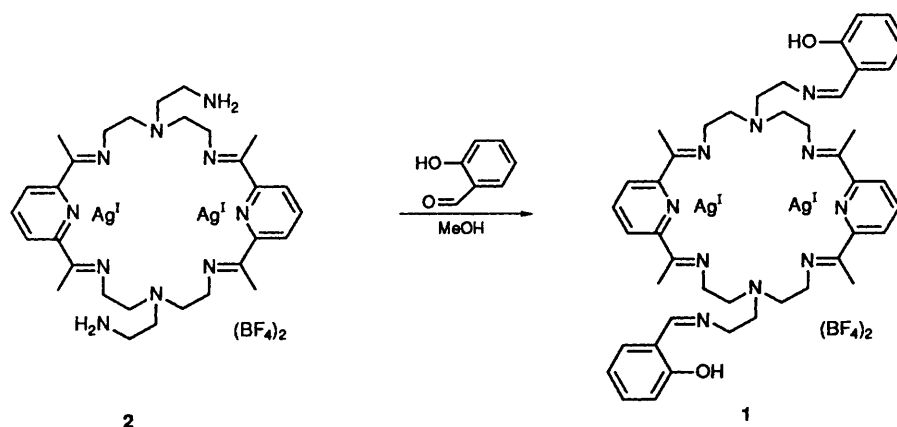
Scheme 2 Transmetalation reactions of the disilver(I) complexes **2** and **3** with copper(II) salts

signal has triplet character as a result of long range coupling [$^5J(\text{H}_c'-\text{H}_r')$ 1.25 Hz] with the methylene group (H_r') adjacent to the imino nitrogen atom, confirmation of which may be derived by irradiation of the methylene signal at δ_{H} 3.31 which causes the methyl triplet to collapse to a singlet. The spectrum was analysed using appropriate decoupling experiments and the $^1\text{H}-^1\text{H}$ shift-correlated (COSY) two-dimensional NMR spectrum; the chemical shift assignments and coupling constants are summarised in Table 5.

The conformationally rigid nature of the macrocycle L^1 in the disilver complex **2** may be demonstrated by variable-temperature ^1H NMR studies, which show the spectrum to be essentially temperature independent in the range 297–228 K. The ^{109}Ag NMR spectrum of **2** recorded at 18.6 MHz in CD_3CN shows a clearly resolved singlet at δ_{Ag} 565 indicative of a single non-labile silver environment in solution. The observed chemical shift value is consistent with those reported for other silver complexes with nitrogen donors²¹ and although the two silver ions were shown to be in close proximity in the crystalline state, no $^{109}\text{Ag}-^{107}\text{Ag}$ coupling arising from the $^{109}\text{Ag}^{107}\text{Ag}$ isotopomer was detected.

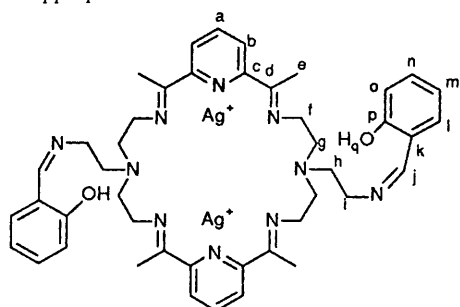
Transmetalation of **2** and **3** with copper(II) salts resulted in the formation of the dinuclear copper(II) species $[\text{Cu}_2\text{L}^1][\text{BF}_4]_4 \cdot 3\text{H}_2\text{O}$ **4** and $[\text{Cu}_2\text{L}^1][\text{ClO}_4]_4 \cdot 2\text{H}_2\text{O}$ **5** (Scheme 2). The spectra of the dinuclear copper(II) complexes are similar to those of the disilver(I) precursors, demonstrating that the macrocycles remain intact during the transmetalation procedure. The most significant differences are an increase in intensity of the bands arising from the counter ions (ca. 1080 and 620 cm^{-1} for ClO_4^- and ca. 1060 cm^{-1} for BF_4^-) and the observation of a broad band around 3400 cm^{-1} indicating the presence of water. The positive ion FAB mass spectra of the dicopper(II) complexes show fragmentation patterns corresponding to the sequential loss of counter ions from the parent molecule **4** ($\text{X} = \text{BF}_4$) $\{[\text{Cu}_2\text{L}^1\text{X}_3]^+ m/z$ 934, $[\text{Cu}_2\text{L}^1\text{X}_2]^+ 847$, $[\text{Cu}_2\text{L}^1\text{X}]^+ 760\}$ and **5** ($\text{X} = \text{ClO}_4$) $\{[\text{Cu}_2\text{L}^1\text{X}_3]^+ m/z$ 971, $[\text{Cu}_2\text{L}^1\text{X}_2]^+ 872$, $[\text{Cu}_2\text{L}^1\text{X}]^+ 771\}$. The nature of the products were also confirmed by elemental analysis. We were unable to grow crystals of these complexes suitable for crystallographic analysis. A study of models built on the premise that the copper atoms were held within the macrocyclic periphery, as were the silver atoms in the precursor complex, indicated that suitable modification of the pendant arms should facilitate the incorporation of a third copper atom leading to the derivation of a trinuclear copper(II) complex in which the metal cluster would be held within the molecular cleft.

Derivatisation of complex **2** was achieved through reaction with salicylaldehyde (Scheme 3) yielding the dinuclear silver(I) complex **1**. It is evident from the IR spectrum that the pendant arms have been functionalised, as a single imine peak of enhanced intensity at 1627 cm^{-1} is present and no primary amine bands are detected. The positive ion FAB mass spectra of **1** show major peaks corresponding to the sequential loss from the parent molecule of first the two perchlorate ions [m/z 1057 (39) and 969 (100%)] and then a single silver ion [m/z 861



Scheme 3 Functionalisation of the pendant arms of the disilver(I) macrocyclic complex 2

Table 6 Proton and ^{13}C NMR assignments of the functionalised disilver complex 1. Labels refer to both carbon and attached hydrogen atoms where appropriate



$\delta(^1\text{H})^a$

H_a	7.99 (2 H, t)	H_j	8.50 (2 H, s)
H_b	7.81 (4 H, d)	H_i	7.04 (2 H, d)
H_c	2.24 (12 H, s)	H_m	6.65 (2 H, t)
H_f	3.64 (8 H, t)	H_n	7.18 (2 H, t)
H_g	3.25 (12 H, br)	H_o	6.56 (2 H, d)
H_h	---	H_q	9.83 (2 H, br)
H_i	3.85 (4 H, br)		

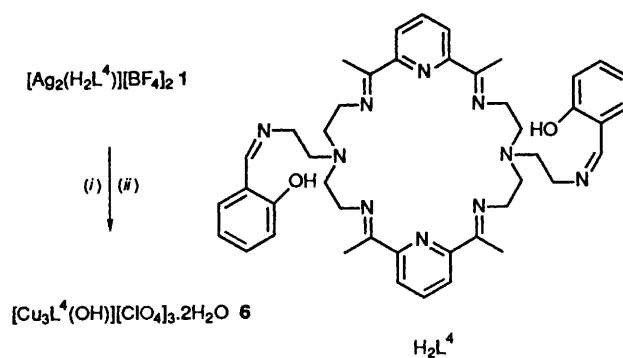
$\delta(^{13}\text{C})^b$

C_a	140.2	C_i	47.7
C_b	124.0	C_j	163.3
C_c	149.5	C_k	120.5
C_d	165.3	C_l	126.6
C_e	15.9	C_m	118.0
C_f	58.0	C_n	132.8
C_g	56.7	C_o	115.9
C_h	54.9	C_p	158.0

^a In $(\text{CD}_3)_2\text{SO}$. Values given as δ (relative integral, multiplicity); s = singlet, d = doublet, t = triplet, br = broad. ^b In $(\text{CD}_3)_2\text{SO}$ at 63 MHz.

(64%). The complex was further characterised by elemental analysis and ^1H and ^{13}C NMR (Table 6). The aromatic and methyl protons gave rise to well resolved signals in contrast to those of the ring and pendant arm methylene groups. This indicates that 1 shows fluxionality at room temperature as compared to the diprimary amine pendant-armed precursor 2. A more thorough investigation of the dynamic processes was precluded by the poor solubility of the complexes in suitable solvents.

Transmetalation of 1 (Scheme 4) was effected by addition of 1 equivalent of copper(II) acetate monohydrate and 2 equivalents of copper(II) tetrafluoroborate hexahydrate to a refluxing solution of 1 in methanol-acetonitrile. The addition of an excess



Scheme 4 Synthesis of the trinuclear copper(II) macrocyclic complex $[\text{Cu}_3\text{L}^4(\text{OH})][\text{ClO}_4]_3 \cdot 2\text{H}_2\text{O}$. (i) $\text{Cu}(\text{MeCO}_2)_2 \cdot \text{H}_2\text{O}$, $2\text{Cu}(\text{BF}_4)_2 \cdot 6\text{H}_2\text{O}$, $\text{MeOH}-\text{MeCN}$, (ii) NaClO_4 , EtOH

of sodium perchlorate led, on cooling, to the isolation of dark green crystals. Elemental analysis indicated the formation of the tricopper(II) hydroxo species $[\text{Cu}_3\text{L}^4(\text{OH})][\text{ClO}_4]_3 \cdot 2\text{H}_2\text{O}$ 6 in which the salicylaldimine pendant arms have been deprotonated. The stability of the $\text{Cu}_3(\text{OH})$ moiety is apparent from the positive ion FAB mass spectrum of the complex in which the two peaks of highest intensity, at m/z 1159 and 1061, correspond to the loss of one and two perchlorate ions respectively from the parent molecule. Additional peaks at m/z 1139, 1042 and 941 arise from cationic species in which the hydroxide ion has also been lost. The source of the hydroxide ion is most likely to be water present in the reaction medium, originating either from the hydration sphere of the copper(II) salts employed in the transmetalation or alternatively from the solvent itself.

X-Ray crystallography confirmed the presence of a discrete trinuclear copper species bound within the macrocyclic framework (Fig. 2). The cluster is comprised of a μ -hydroxo-bridged pair, Cu(1) and Cu(2), and a non-bridged copper atom Cu(3). The two metal ions of the dinuclear moiety are separated by 3.62 Å with a Cu(1)–O(H1)–Cu(2) angle of 138.2°. A scalene triangular array is completed by the third copper atom Cu(3) with Cu(1) \cdots Cu(3) and Cu(2) \cdots Cu(3) distances of 5.89 and 4.95 Å respectively.

The co-ordination geometries around the copper atoms of the hydroxo-bridged pair, Cu(1) and Cu(2), may be described as distorted square-based pyramidal. The basal donors of the former are provided by the nitrogen atoms, N(1), N(2) and N(8), of one pyridine diimine unit and the bridging hydroxide O(H1). The axial site is filled by the oxygen atom O(S1) of a water molecule. The other copper atom, Cu(2), of the dinuclear moiety is co-ordinated by the donor atoms, O(2) and N(10), of a salicylaldimine pendant arm, a tertiary amino nitrogen N(7) of the macrocyclic ring, the bridging hydroxide O(H1) and one of the imine nitrogen atoms N(6) of the second pyridine diimine unit.

The third copper atom Cu(3) also has a distorted square-

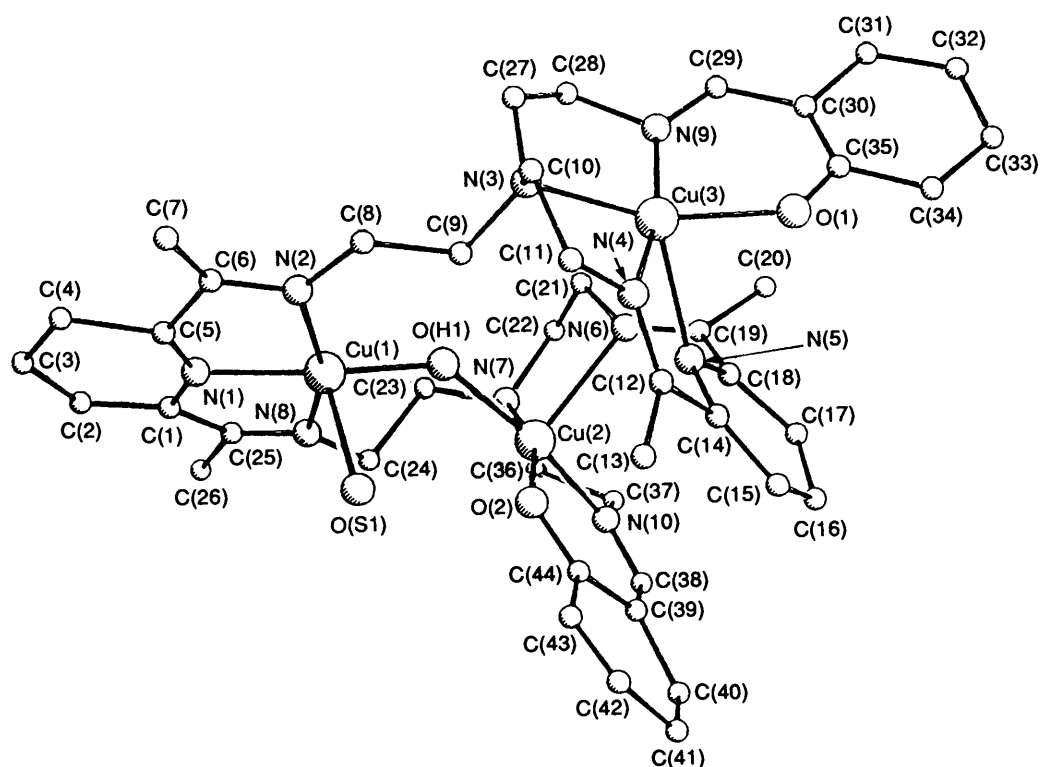


Fig. 2 The molecular structure of the $[\text{Cu}_3\text{L}^4(\text{OH})]^{3+}$ in complex 6

Table 7 Co-ordination geometry about atoms Cu(1), Cu(2) and Cu(3) in complex 6; bond lengths in Å, other entries are the angles (°) subtended at copper by the atoms in the first column and the bottom row

Cu(1)–O(H1)	1.880(19)				
Cu(1)–O(S1)	2.243(24)	86.3(9)			
Cu(1)–N(1)	2.002(24)	167.5(8)	104.5(9)		
Cu(1)–N(2)	2.166(26)	106.5(9)	90.7(10)	80.1(10)	
Cu(1)–N(8)	2.040(24)	91.4(9)	100.4(11)	80.5(10)	159.6(13)
		O(H1)	O(S1)	N(1)	N(2)
Cu(2)–O(H1)	1.995(20)				
Cu(2)–N(6)	2.294(31)	91.9(10)			
Cu(2)–N(7)	2.154(26)	89.8(10)	80.5(10)		
Cu(2)–N(10)	1.964(33)	169.6(11)	96.0(12)	84.9(12)	
Cu(2)–O(2)	1.905(20)	87.9(9)	118.4(10)	161.1(11)	94.3(11)
		O(H1)	N(6)	N(7)	N(10)
Cu(3)–N(3)	2.050(27)				
Cu(3)–N(4)	1.955(24)	77.3(11)			
Cu(3)–N(5)	2.283(25)	121.9(9)	76.5(9)		
Cu(3)–N(9)	1.949(26)	89.4(11)	165.1(12)	116.9(9)	
Cu(3)–O(1)	2.003(24)	155.0(9)	99.9(10)	80.5(9)	89.3(10)
		N(3)	N(4)	N(5)	N(9)

pyramidal co-ordination environment derived from the donors, O(1) and N(9), of the second pendant arm, a tertiary amino nitrogen N(3), together with the remaining imine nitrogen N(4) from the second macrocyclic head unit and a pyridyl nitrogen N(5). The co-ordination mode of the pyridyl nitrogen N(5) to the copper ion Cu(3) is unusual since the copper atom lies 1.17 Å out of the plane of the pyridine ring; thus the nitrogen lone pair does not point directly at the metal ion. The bond lengths and bond angles defining the co-ordination geometries around the three copper atoms in 6 are presented in Table 7.

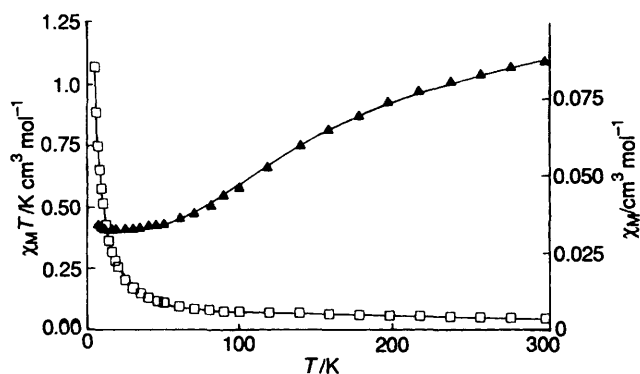
The macrocycle adopts a twisted conformation in which the two planar pyridyl units [1: N(1), C(1), C(2), C(3), C(4) and C(5); 2: N(5), C(14), C(15), C(16), C(17) and C(18); r.m.s. deviations 0.024 and 0.049 Å respectively] are inclined at 64°. Co-ordination of the two planar salicylideneimine pendant groups [1: N(9)–O(1); 2: N(10)–O(2); r.m.s. deviations of six-

membered rings 0.042 and 0.054 Å respectively] by the two copper atoms Cu(2) and Cu(3) is facilitated by a bending of the macrocycle away from the cleft conformation exhibited in earlier structures. A molecular cleft, with an average interplanar separation of 3.37 Å and interplanar inclination angle between six-membered rings of 4.8°, is formed between the second pendant salicylideneimine unit and the second pyridyl ring. One of the perchlorate anions is weakly co-ordinated to a copper atom, while the other anions are involved in a hydrogen-bonding network with the disordered water molecules. The chiral conformations of the chelate rings Cu(2)–N(6)–C–N(7)–C–C–N(10) and Cu(3)–N(4)–C–C–N(3)–C–C–N(9) are $\delta\delta$ and $\delta\lambda$. Intermolecular and intramolecular hydrogen bonds are present between the salicylideneimine oxygen atoms, O(1) and O(2), and the copper-co-ordinated water molecule, O(S1), and intermolecular copper distances for 6 are Cu(1)...

Table 8 Magnetic and structural parameters for $[\text{Cu}_3\text{L}^4(\text{OH})]^{3+}$ **6** and related mono-hydroxo-bridged dicopper(II) complexes [fuller compilations of mono-hydroxo-bridged dicopper(II) complexes having Cu–O–Cu angles in the range 100–145° are given in ref. 27]

Complex cation ^a	$-2J/\text{cm}^{-1}$	$\theta(\text{Cu}-\text{O}-\text{Cu})/^\circ$ ^b	$r(\text{Cu}-\text{O})/\text{\AA}$ ^c	$\text{Cu}\cdots\text{Cu}/\text{\AA}$	Ref.
$[\text{Cu}_2\text{L}^5(\text{OH})]^{3+}$	820	132	1.85	3.38	23
$[\text{Cu}_3\text{L}^4(\text{OH})]^{3+}$	202	138	1.88, 1.99	3.57	This work
$[\text{Cu}_2(\text{dpm})_2(\text{tpe})(\text{OH})]^{3+}$	360	138	1.96	3.66	27
$[\text{Cu}_2(\text{bipy})_4(\text{OH})]^{3+}$	322	142	1.93	3.65	25
$[\text{Cu}_2\text{L}^6(\text{OH})]^{3+}$	240	142	1.87, 1.91	3.57	26
$[\text{Cu}_2\text{L}^7(\text{OH})(\text{ClO}_4)]^{2+}$	1000	144	1.92	3.64	24

^a $\text{L}^5 = 1,4$ -bis[(1-oxa-4,10-dithia-7-azacyclododecan-7-yl)methyl]benzene, tpe = 1,1,2-tetrakis(2-pyridyl)ethane, dpm = di(2-pyridyl)methane, bipy = 2,2'-bipyridine, $\text{L}^6 =$ macrocycle derived from the condensation of 2,6-diacetylpyridine and 3,6-dioxaoctane-1,8-diamine, $\text{L}^7 =$ sexadentate macrocycle, 1,13-dioxa-4,7,10,16,19,22-hexazacyclotetrasane. ^b θ is the angle subtended by the copper atoms at the bridging ligand. ^c Copper-hydroxo ligand bond length.

**Fig. 3** The variation with temperature (T) of the molar susceptibility χ_M (\square) and the product $\chi_M T$ (\blacktriangle) for complex **6**

$\text{Cu}(3^i)$ 6.06 and $\text{Cu}(2) \cdots \text{Cu}(3^i)$ 6.53 \AA ($i: -x, y - 0.5, -z$).

The UV/VIS spectrum of the trinuclear copper(II) complex **6** is dominated by an intense absorption with λ_{max} at 376 nm. The high molar extinction coefficient ($\epsilon = 7400 \text{ dm}^3 \text{ mol}^{-1} \text{ cm}^{-1}$) of this band indicates that it arises as a result of ligand-to-metal charge transfer. No such feature is observed in the absorption spectra of **5**; thus it appears that this electronic transition originates from interaction with either a deprotonated phenolic oxygen atom or from the hydroxide ion. A lower intensity broad band with λ_{max} at 627 nm ($\epsilon = 440 \text{ dm}^3 \text{ mol}^{-1} \text{ cm}^{-1}$) is assigned as d–d in character, but the spectral region of most relevance to ascorbate oxidase,²² at ca. 330 nm, is obscured by the intense absorption of the ligand π system.

The electron spin resonance (ESR) spectrum of **6** is relatively uninformative. The solid-state spectrum recorded at 3.8 K shows a single broad signal with no discernible hyperfine coupling. The observed g value of 2.107 is consistent with that derived from the magnetic studies. At higher temperatures the signal is further broadened reflecting the partial population of the triplet state of the dicopper moiety. Repetition of the ESR experiment in frozen acetonitrile solution at 128 K did not yield any additional information.

Magnetic susceptibility measurements carried out on **6** are consistent with a system composed of an antiferromagnetically coupled copper(II) pair and a third magnetically independent copper(II) ion. The magnetic behaviour of **6** is illustrated in Fig. 3 as the temperature dependence of the molar susceptibility and of the $\chi_M T$ product over the range 5–300 K. The latter exhibits a plateau at $\chi_M T \approx 0.4 \text{ K cm}^3 \text{ mol}^{-1}$ at low temperature ($T < 25 \text{ K}$) and then an increase with temperature until $\chi_M T = 1.09 \text{ K cm}^3 \text{ mol}^{-1}$ at 300 K. On the other hand the low-temperature value clearly identifies a $S = \frac{1}{2}$ ground state.

Owing to the long distances from $\text{Cu}(3)$ to the pair of copper atoms the data have been analysed using equation (1)

$$\chi_M = (2N\beta^2 g_1^2 / kT) [3 + \exp(-2J/kT)]^{-1} + N\beta^2 g_2^2 / 3k(T - \theta) + \text{t.i.p.} \quad (1)$$

in which the first (Bleaney–Bowers) term and the second (Curie) term account for the pair [$\text{Cu}(1)$, $\text{Cu}(2)$] and for $\text{Cu}(3)$ respectively. It was necessary to include a Weiss constant (θ) in the Curie expression to account for the small increase of $\chi_M T$ at the lowest temperatures; t.i.p. represents the temperature independent paramagnetism. The best fit of the data was obtained with the following values for the parameters; $g_1 = 2.063$, $g_2 = 2.056$, $2J = -202 \text{ cm}^{-1}$, $\theta = 0.32 \text{ K}$, t.i.p. = $4.4 \times 10^{-4} \text{ cm}^3 \text{ mol}^{-1}$. The use of the different Landé factors g_1 and g_2 is justified by the different environments of $\text{Cu}(3)$ and of the copper atoms of the pair. The excellent agreement between the experimental data and the theoretical values justifies the validity of the model. Lastly it must be noted that the small ferromagnetic interaction discernible at $T < 12 \text{ K}$ ($\theta = 0.32 \text{ K}$) cannot be due to an intramolecular interaction between $\text{Cu}(3)$ and the pair since at these temperatures the $S = 1$ level of the pair is not populated. It therefore reflects intermolecular interactions between $\text{Cu}(3)$ atoms from neighbouring molecules. Accordingly the three-copper unit can be described as a mononuclear site non-interacting with a moderately coupled copper pair ($2J = -202 \text{ cm}^{-1}$).

There is a limited number of mono- μ -hydroxo dicopper complexes^{23–26} and no magnetostructural correlation emerges from their comparison (Table 8). Owing to the tetragonal environment of $\text{Cu}(1)$ and $\text{Cu}(2)$ the metallic component of their magnetic orbitals will be $d_{x^2 - y^2}$ which points towards the equatorial ligands. As a consequence strong overlap is expected with the hydroxo-bridge. The high value of the Cu–O–Cu angle (137.8°) should give rise to a strong antiferromagnetic interaction but the long Cu(2)–OH bond (1.995 \AA) counterbalances this effect and a moderate interaction is observed ($2J = -202 \text{ cm}^{-1}$). The origin of this elongated Cu–O bond is to be found in its *trans* position relative to the Cu–N imine bond. The strong binding of the salicylaldimine moiety [$\text{Cu}(2)$ –O(2) 1.905, $\text{Cu}(2)$ –N(10) 1.964 \AA] induces a weakening of the two other equatorial bonds [$\text{Cu}(2)$ –N(7) 2.154, $\text{Cu}(2)$ –O(H1) 1.995 \AA].

Conclusion

The [2 + 2] cyclocondensation of 2,6-diacetylpyridine and tris(2-aminoethyl)amine in the presence of silver(I) ions provides a useful route for the high yield synthesis of a dinucleating Schiff-base macrocycle L^1 bearing two primary amine pendant arms. The macrocyclic imine bonds are relatively stable and functionalisation of the pendant arms may be effected through further condensation reactions with aromatic carboxaldehydes.

The salicylaldehyde derivative **1** of the disilver diprimary amine pendant-armed complex **2** may be transmetalated with copper(II) salts yielding the trinuclear complex $[\text{Cu}_3\text{L}^4(\text{OH})][\text{ClO}_4]_3 \cdot 2\text{H}_2\text{O}$ **6**, the structure of which shows a trinuclear copper(II) cluster held within the ligand perimeter. The cluster is comprised of a Type 2-like copper atom and a Type 3-like centre. The Type 2 atom is 4.9 and 5.9 \AA distant from the two copper

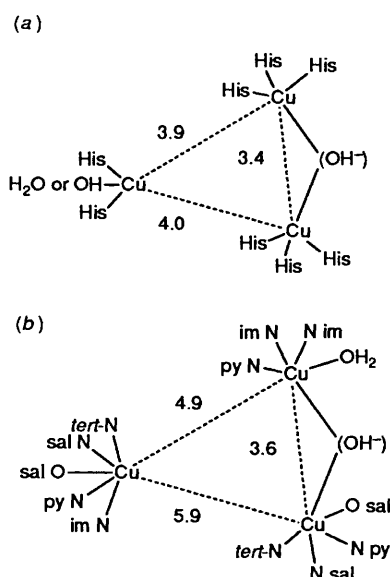


Fig. 4 A comparison of the trinuclear copper co-ordination sites in ascorbate oxidase (a) and the model complex **6** (b). His = histidyl residue, im N = imine nitrogen, py N = pyridyl nitrogen, sal N = salicyl nitrogen, sal O = salicyl oxygen, tert-N = tertiary amine nitrogen; distances in Å

atoms of the Type 3 centre. The two copper atoms of this centre are 3.6 Å apart and bridged by a hydroxy group the origin of which appears to be water from the reaction medium with the two copper(II) atoms acting in concert as a superacid pair to promote the generation of a nucleophile. There are significant differences between the co-ordination geometries found in **6** and the metallobiosite (Fig. 4); the detection of a hydroxo-bridge in **6** does however give credence to the notion that the bridge in ascorbate oxidase is of the same type. The presence of the hydroxo-bridge reinforces the statement made by Coughlin and Lippard²⁴ that the stability and ubiquity of the $\text{Cu}_2(\text{OH})^{3+}$ moiety (as detected in Type 3 centre models) suggests that the endogenous bridging protein ligand proposed for Type 3 biosites might simply be the hydroxide anion itself, generated from accompanying water molecules.

The trinuclear copper(II) complex cannot be claimed to provide a precise replication of the ascorbate oxidase cluster; the co-ordination spheres of the metal ions differ both in terms of the nature and the geometric arrangement of the donor atoms. The small molecule derived clef has a greater degree of conformational freedom than the more highly defined proteinaceous clefts and so the need to design in features to constrain this mobility is apparent. The trinuclear copper(II) complex does however serve as a first-generation model for a Type 3 oxidase site in that it reproduces features of the biosite to a greater extent than any synthetic complex previously reported. It also provides food for thought with respect to the comparative identity of the Type 3 sites in haemocyanins and 'blue' oxidases—are they similar as suggested from extended X-ray absorption fine structure (EXAFS) studies on haemocyanins and tyrosinase or are they different as hinted at by studies on small molecule models?

Acknowledgements

We thank the SERC for grants (to P. C. H. and P. D. H.), the SERC and the Royal Society for support and assistance in the purchase of the diffractometer and the EEC for support through contract number SC1-0167-C(A).

References

- 1 R. Malkin and B. G. Malmström, *Adv. Enzymol. Relat. Areas Mol. Biol.*, 1970, **33**, 177; B. G. Malmström, L.-E. Andréasson and B.

- Reinhammer, in *The Enzymes*, ed. P. D. Boyer, Academic Press, New York, 1975, vol. 9; E. I. Solomon, K. W. Penfield and D. E. Wilcox, *Struct. Bonding (Berlin)*, 1983, **53**, 1.
- 2 J. A. Fee, *Struct. Bonding (Berlin)*, 1975, **23**, 1.
- 3 B. G. Malmström, *Ann. Rev. Biochem.*, 1982, **51**, 21.
- 4 K. G. Strothkamp, C. R. Dawson, *Biochemistry*, 1974, **13**, 434.
- 5 J. L. Cole, G. O. Tan, E. K. Yang, K. O. Hodgson and E. I. Solomon, *J. Am. Chem. Soc.*, 1990, **112**, 2243; J. L. Cole, P. A. Clark and E. I. Solomon, *J. Am. Chem. Soc.*, 1990, **112**, 9534; J. L. Cole, L. Avigliano, L. Morpugno and E. I. Solomon, *J. Am. Chem. Soc.*, 1991, **113**, 9080.
- 6 (a) A. Messerschmidt, A. Rossi, R. Ladenstein, R. Huber, M. Bolognesi, G. Gatti, A. Marchesini, R. Petruzelli and A. Finazzo-Agró, *J. Mol. Biol.*, 1989, **206**, 513; (b) A. Messerschmidt, R. Ladenstein, R. Huber, M. Bolognesi, L. Avigliano, R. Petruzelli, A. Rossi and A. Finazzo-Agró, *J. Mol. Biol.*, 1992, **224**, 179.
- 7 J. Li, D. R. McMillan and W. E. Antholine, *J. Am. Chem. Soc.*, 1992, **114**, 725.
- 8 A. Messerschmidt and R. Huber, *Eur. J. Biochem.*, 1990, **187**, 341.
- 9 R. Beckett and B. F. Hoskins, *J. Chem. Soc. Dalton Trans.*, 1972, 291; P. V. Ross, R. K. Murmann and E. O. Schlemper, *Acta Crystallogr., Sect. B*, 1974, **30**, 1120; R. J. Butcher, C. J. O'Connor and E. Sinn, *Inorg. Chem.*, 1981, **20**, 537; F. B. Hulsbergen, R. W. M. ten Hoedt, G. C. Verschoor, J. Reedijk and A. L. Spek, *J. Chem. Soc., Dalton Trans.*, 1983, 539; J. P. Costes, F. Dahan and J. P. Laurent, *Inorg. Chem.*, 1986, **25**, 413; S. Baral and S. Chakravorthy, *Inorg. Chim. Acta.*, 1980, **39**, 1; N. A. Bailey, D. E. Fenton, R. Moody, P. J. Scrimshire, E. Beloritzky, P. H. Fries and J. M. Latour, *J. Chem. Soc., Dalton Trans.*, 1988, 2817.
- 10 J. Comarmond, B. Dietrich, J.-M. Lehn and R. Louis, *J. Chem. Soc., Chem. Commun.*, 1985, 74.
- 11 K. D. Karlin, Q.-F. Gan, A. Farooq, S. Liu and J. Zubieta, *Inorg. Chem.*, 1990, **29**, 2549.
- 12 H. Adams, N. A. Bailey, D. E. Fenton, W. D. Carlisle and G. Rossi, *J. Chem. Soc., Dalton Trans.*, 1990, 1271.
- 13 H. Adams, N. A. Bailey, M. J. S. Dwyer, D. E. Fenton, P. C. Hellier and P. D. Hempstead, *J. Chem. Soc., Chem. Commun.*, 1991, 1297.
- 14 J. D. Crane, D. E. Fenton, J. M. Latour and A. J. Smith, *J. Chem. Soc., Dalton Trans.*, 1991, 2979.
- 15 N. A. Bailey, D. E. Fenton, P. C. Hellier, P. D. Hempstead, U. Casellato and P. A. Vigato, *J. Chem. Soc., Dalton Trans.*, 1992, 2809.
- 16 *International Tables for X-Ray Crystallography*, Kynoch Press, Birmingham, 1974, vol. 4.
- 17 G. M. Sheldrick, SHELXTL, An integrated system for solving, refining and displaying crystal structures from diffraction data (Revision 4), University of Göttingen, 1983.
- 18 D. E. Fenton and G. Rossi, *Inorg. Chim. Acta*, 1985, **98**, L29.
- 19 M. G. B. Drew, S. G. McFall, S. M. Nelson and C. P. Waters, *J. Chem. Res.*, 1979, (S) 16; (M) 360; S. M. Nelson, *Pure Appl. Chem.*, 1980, **52**, 2461.
- 20 J. Jazwinski, J.-M. Lehn, D. Lilienbaum, R. Ziessel, J. Guilheim and C. Pascard, *J. Chem. Soc., Chem. Commun.*, 1987, 1691; D. McDowell and J. Nelson, *Tetrahedron Lett.*, 1988, 385; M. G. B. Drew, D. McDowell and J. Nelson, *Polyhedron*, 1988, **7**, 2229; V. McKee, W. T. Robinson, D. McDowell and J. Nelson, *Tetrahedron Lett.*, 1989, 7453; D. McDowell, J. Nelson and V. McKee, *Polyhedron*, 1989, **8**, 1143; M. G. B. Drew, D. Marrs, J. Hunter and J. Nelson, *J. Chem. Soc., Dalton Trans.*, 1992, 11.
- 21 R. J. Goodfellow, in *Multinuclear NMR*, ed. J. Mason, Plenum Press, New York, 1987, ch. 21; P. M. Hendricks, in *NMR of Newly Accessible Nuclei*, ed. P. Laszlo, Academic Press, London, 1983, ch. 12.
- 22 C. D. LuBien, M. E. Winkler, T. J. Thamann, R. A. Scott, M. S. Co, K. O. Hodgson and E. I. Solomon, *J. Am. Chem. Soc.*, 1981, **103**, 7014; D. J. Spira-Solomon and E. I. Solomon, *J. Am. Chem. Soc.*, 1987, **109**, 6421; L.-S. Kau, D. J. Spira-Solomon, J. E. Penner-Hahn, K. O. Hodgson and E. I. Solomon, *J. Am. Chem. Soc.*, 1987, **109**, 6433.
- 23 P. L. Burk, J. A. Osborn, M. T. Youinou, Y. Agnus, R. Louis and R. Weiss, *J. Am. Chem. Soc.*, 1981, **103**, 1273.
- 24 P. K. Coughlin and S. J. Lippard, *J. Am. Chem. Soc.*, 1981, **103**, 3228.
- 25 S. R. Haddad, S. R. Wilson, D. J. Hodgson and D. N. Hendrickson, *J. Am. Chem. Soc.*, 1981, **103**, 384.
- 26 M. G. B. Drew, M. McCann and S. M. Nelson, *J. Chem. Soc., Dalton Trans.*, 1981, 1868.
- 27 L. K. Thompson, F. W. Hartstock, P. Robichaud and A. W. Hanson, *Can. J. Chem.*, 1984, **62**, 2755; L. K. Thompson, F. L. Lee and E. J. Gabe, *Inorg. Chem.*, 1988, **27**, 39.

Received 20th October 1992; Paper 2/05593G